



Deep Transfer Learning Networks for Brain Tumor Detection: The Effect of MRI Patient Image Augmentation Methods

Peshraw Ahmed Abdalla*

University of Halabja, Halabja 46018,
Kurdistan Region, IRAQ

Abdalbasit Mohammed Qadir

University of Human Development,
Sulaimaniyah 46001, Kurdistan Region, IRAQ

Omed Jamal Rashid

University of Halabja, Halabja
46018, Kurdistan Region, IRAQ

Karwan M. Hama Rawf

University of Halabja, Halabja 46018,
Kurdistan Region, IRAQ

Ayub O. Abdulrahman

University of Halabja, Halabja
46018, Kurdistan Region, IRAQ

Bashdar Abdalrahman Mohammed

University of Halabja, Halabja 46018, Kurdistan Region,
IRAQ

Article Info

Article history:

Received: October 6, 2022

Revised: November 20, 2022

Accepted: December 31, 2022

Keywords:

Artificial intelligence;
cancer detection;
deep learning;
denseNet201;
mobileNetV2;
VGG19; MRI.

Abstract

The exponential growth of deep learning networks has enabled us to handle difficult tasks, even in the complex field of medicine with small datasets. In the sphere of treatment, they are particularly significant. To identify brain tumors, this research examines how three deep learning networks are affected by conventional data augmentation methods, including MobileNetV2, VGG19, and DenseNet201. The findings showed that before and after utilizing approaches, picture augmentation schemes significantly affected the networks. The accuracy of MobileNetV2, which was originally 85.33%, was then enhanced to 96.88%. The accuracy of VGG19, which was 77.33%, was then enhanced to 95.31%, and DenseNet201, which was originally 82.66%, was then enhanced to 93.75%. The models' accuracy percentage engagement change is 13.53%, 23.25%, and 23.25%, respectively. Finally, the conclusion showed that applying data augmentation approaches improves performance, producing models far better than those trained from scratch.

To cite this article: P. A. Abdalla, A. M. Qadir, O. J. Rashid, K. M. H. Rawf, A. O. Abdulrahman, and B. A. Mohammed, "Deep Transfer Learning Networks for Brain Tumor Detection: The Effect of MRI Patient Image Augmentation Methods," *Int. J. Electron. Commun. Syst.*, vol. 2, no. 2, pp. 39-48, 2022.

INTRODUCTION

Despite the sophistication of modern medical research, some diseases are still difficult for doctors to recognize early. Doctors use brain tomography images and magnetic resonance imaging (MRI) to detect brain tumors. A variety of patients can be seen in these pictures. Identifying the problem early is necessary for the benefit of patients. Brain tumors are a very grave and potentially lethal type of cancer. The two known illnesses are Low-Grade Glioma (LGG) and High-Grade Glioma (HGG). After diagnosis, people with HGG have an average lifetime of 14 months. There are many ways to cure diseases, including chemotherapy and radiotherapy [1].

Usually, surgery is utilized to try and address this condition. This happens as a result of the tumor pressing against the brain.

Because brain tumors are situated in the skull, their appearance might vary depending on how the pressure changes. Severe headache, nausea, and vomiting are some of the most important symptoms. Patients with the syndrome may occasionally develop circulation issues and possibly undergo paralysis.

Additionally, the symptoms differ depending on which brain area is affected. These symptoms range from speech difficulties to numbness to eyesight and hearing loss to irregular gait. It is unclear what specifically causes brain tumors. Deep learning and machine learning techniques are used in many fields nowadays [2-6]. This system can be made accessible worldwide by various technologies, including IoT and cloud-based systems [7-9].

• Corresponding author:

Peshraw Ahmed Abdalla, Computer Science Department, College of Science, University of Halabja, Halabja 46018, Kurdistan Region, IRAQ. ✉ peshraw.abdalla@uoh.edu.iq

© 2022 The Author(s). **Open Access.** This article is under the CC BY SA license (<https://creativecommons.org/licenses/by-sa/4.0/>)

Nevertheless, it cannot be denied that persons of all ages can get brain tumors. The prevalence of this illness will rise as the world's population ages [10]. The seriousness of the issue makes brain tumor diagnosis a particularly active field of study [11]. This study developed a method for assisting doctors in disease identification using a set of publicly available MRI images [12]. The study also aims to help people who live in rural areas without access to specialist medical care diagnose brain tumor illnesses early. Once more, this study aims to prevent doctors from misdiagnosing patients when they are exhausted and overworked.

The innovative contributions made by this research work include the following: 1) Traditional methods for data augmentation are described; 2) The application of data augmentation techniques result in a framework for assessing the efficacy of multiple models; 3) To determine how image augmentation techniques with limited datasets boost the improvement in accuracy percentage, the performance of convolutional neural networks like MobileNetV2, VGG19, and DenseNet201 is compared. The Effect of MRI Patient Image Augmentation Methods [13]. The models' performance was compared before and after applying image augmentation techniques, and several metrics, including accuracy, precision, recall, and f1 score, were used to assess the models' performance.

In the literature, there is a wide range of studies on brain tumor identification. Dong et al. suggested a reliable segmentation method for automatically segmenting brain tumors. They used the BRATS2015 dataset for their study. They claimed that their advised strategy resulted in favorable effects [14]. An automatic technique that can determine whether or not the brain has a tumor from MRI data was presented by Amin et al. The research used local, Harvard, and Rider databases; the highest level of accuracy was 97.1 percent [15]. Wu et al. proposed a color-based segmentation to identify brain cancers, using K-means clustering as the method. They asserted that the method could successfully divide MRI images of brain tumors, enabling pathologists to precisely determine the size and location of lesions [16]. Chandra et al. proposed a prototype for locating brain

cancers. This model is based on a genetic algorithm [17].

Recent research findings are promising and have numerous implications for detecting and managing brain tumors. Nevertheless, despite the encouraging results that the authors highlight, many limitations prevent much research from being valid in the real clinical environment. Because of the limited access and the small amount of data used to train the models, the authors emphasize that the findings cannot be more accurate. For example, Olin et al. claim that the models were created using a single study with a maximum of 800 pictures and tiny patient datasets for head and neck illnesses [18].

However, Jayachandran et al. report only 775 cases of glioblastoma [19]. Amemiya et al. make a similar argument, claiming that their study of 127 patients had insufficient data and that additional data might produce better results [20]. Tandel et al. can only investigate 130 individuals with brain tumors, but they work over this limitation by using transfer learning, picture scaling, rotation, and data augmentation [21]. Jiang et al. also increase the quality of the models by flipping, resizing, and smoothing the photographs [22]. Wang et al. use image warping, flipping, rotation, and the gamma function to change their images' color (contrast) in a manner similar to this [23]. The apps were implemented utilizing moderate data, but no learning transfer or data augmentation methods were used. Al-Saffar and Menze are two examples of them [24, 25]. The research presented makes it quite clear. The few studies that use data augmentation also neglect to present the results before and after applying the approaches.

By offering thorough information on detecting brain tumors, this study seeks to cover research gaps and contribute to the research field and serve as a platform for primary probabilistic research by using Deep Transfer Learning Networks for Brain Tumor Detection with three transfer learning models were used to identify brain tumors in MRI images.

METHODS

The networks employed, the picture augmentation methods used, and the dataset used for this study are all explained in this section. The appropriate course of action must be decided based on the type of tumor, its

location, size, and the degree of brain and nerve damage it has caused. The information hidden in the MRI images must be made public to detect tumors early.

Data Set

The experiments' publicly accessible dataset was taken from Kaggle [26]. This data set consists of two classes. There is no tumor in the top-notch data. The second data class consists of pictures of the patient with the tumor. The MRI images in Figure 1 show a healthy person on the left. Figure 1 on the right once more displays MRI scans of a patient with a brain tumor. The dataset is divided into two parts: the first portion contains 70% of the MTI images for the training phase, and the second part, 30%, is used to test the models before and after using image augmentation techniques, as shown in Figure 2.

Image Enhancement techniques

Several methods, from simple modifications like geometric adjustments to complex mosaic-based visuals, have been developed due to deep learning networks' inherent need for enormous volumes of data.

- Random deletion of frames
- Translation, Rotation, and Flip
- Resizing and Cropping
- Image overlay and Noise injection
- Distortion
- Colour space and Linear filters

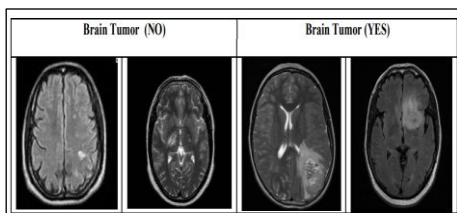


Figure 1. Brain Scans with MRI

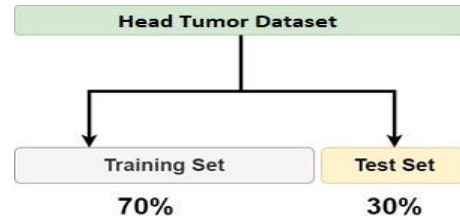


Figure 2. The Dataset's Precise Distribution

Around 86 percent of the data augmentation approaches utilized in deep learning in medical imaging fall under the categories of "basic" and/or "deformable" techniques [27].

Deep Learning Architectures

Deep learning is built on artificial neural networks and computer programs that mimic the functions of the human brain. Deep learning is built on machine learning principles. Deep learning uses many layers to convert and extract features. Each layer takes the output of the layer before it as input [28]. Although there are other deep learning designs, the following networks were used in this study:

MobileNetV2

The 53 layers of MobileNetV2 are convolutional neural networks. A pre-trained network using more than a million images in the ImageNet database is available for loading. The pre-trained network is capable of classifying photos into 1000 different object categories. This result has led to network learning detailing a range of image representations with features. The network's picture input is 224×224 pixels. The architecture of the MobileNetV2 is demented in Figure 3.

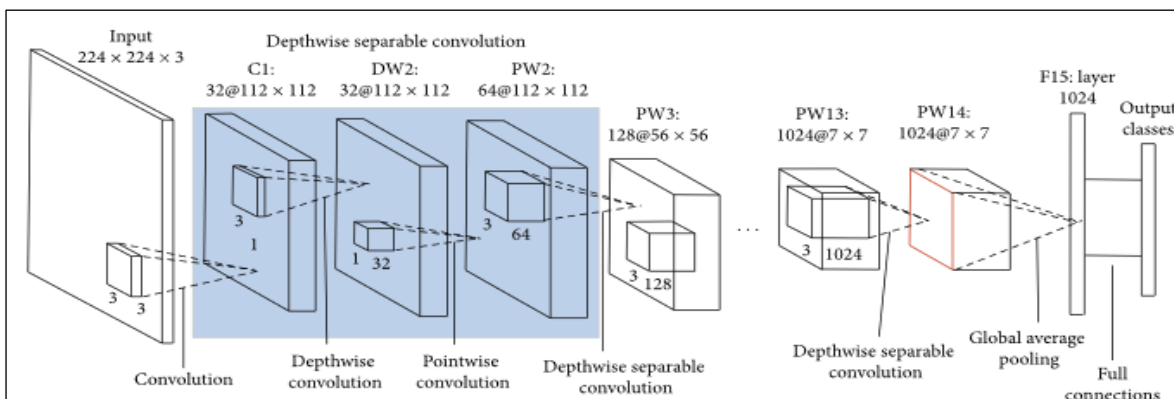


Figure 3. The MobileNetV2's architecture

VGG19

There are 19 layers in the convolutional neural network known as VGG-19. A network that has been pre-trained using the ImageNet database's more than a million images is available for loading. The pre-trained network is capable of classifying photos into 1000 different object categories, including keyboard,

mouse, pencil, and numerous animal images. This ability has led to the network learning detailed feature representations for various images. A 224 by 224 pixels image can be entered into the network [29]. The architecture of the VGG19 is demonstrated in Figure 4 [30].

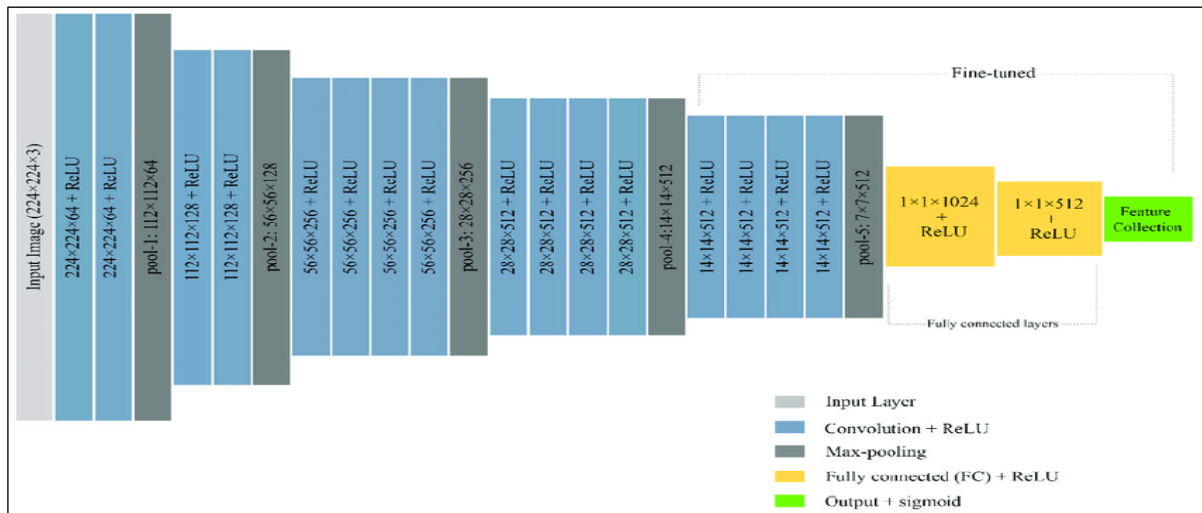


Figure 4. The VGG19's Architecture

DenseNet201

A convolutional neural network of 201 layers deep is called DenseNet201. A pre-trained network version trained on more than one million photographs is available in the ImageNet database. Using the pre-trained network, one thousand different object

categories can be identified in pictures. As a result, the network has collected extensive feature representations for a range of photos. The network can accept images up to 224 by 224 pixels [31]. The architecture of the DenseNet201 is demented in Figure 5.

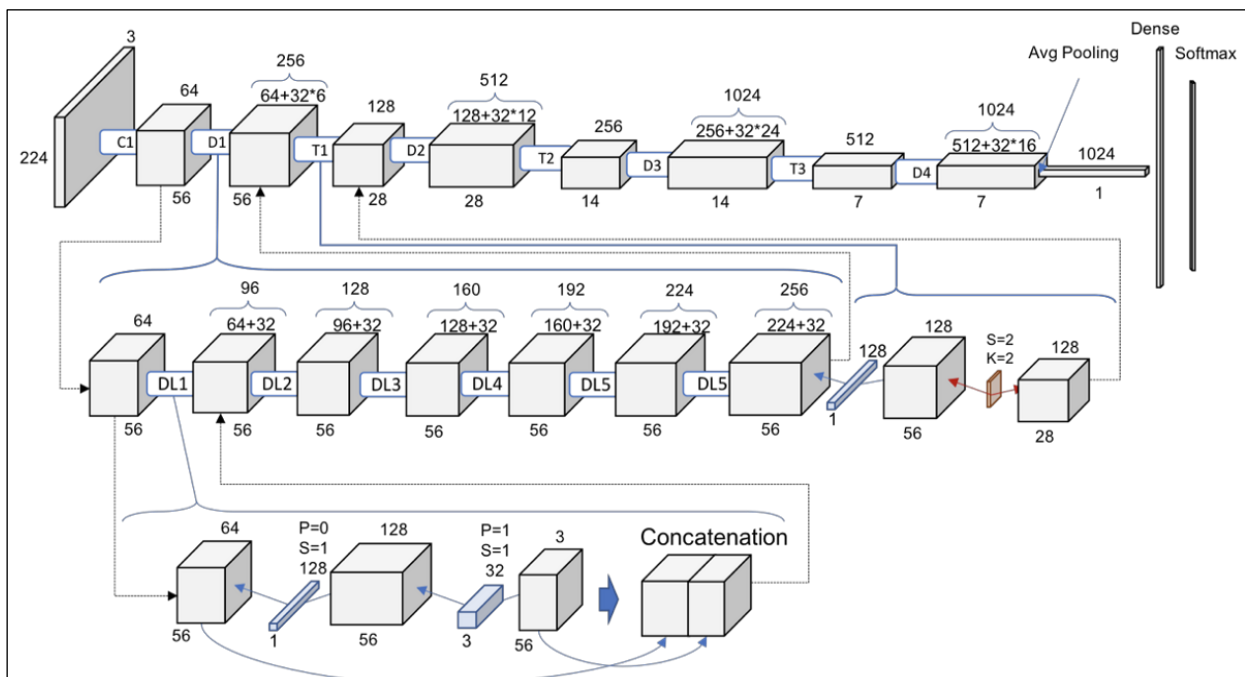


Figure 5. The DenseNet201's Architecture

RESULTS AND DISCUSSION

A common visual representation of the effectiveness of classification methods is a confusion matrix. The matrix (table) displays the proportion of correctly and wrongly identified instances in the test data compared to the actual results (target value). One benefit of using a confusion matrix (CM) as an approach for evaluation is that it enables more comprehensive analysis (such as when the model confuses two classes), as opposed to just looking at the proportion of examples that were correctly classified, which can produce false results if the dataset is unbalanced [32]. Figure 6 explains a confusion matrix [33].

		Predicted Class		
		Positive	Negative	
Actual Class	Positive	True Positive (TP)	False Negative (FN) Type II Error	Sensitivity $\frac{TP}{(TP + FN)}$
	Negative	False Positive (FP) Type I Error	True Negative (TN)	Specificity $\frac{TN}{(TN + FP)}$
		Precision $\frac{TP}{(TP + FP)}$	Negative Predictive Value $\frac{TN}{(TN + FN)}$	Accuracy $\frac{TP + TN}{(TP + TN + FP + FN)}$

Figure 6. A confusion matrix

For more explanation, we used several metrics such as specificity, sensitivity, negative predictive value, precision, false discovery rate, false positive rate, accuracy, false negative rate, f1 score, and Matthews correlation coefficient.

Accuracy

Through the use of CM parameters, accuracy can be determined. The entire quantity of accurate predictions is divided by the total quantity of forecasts in this case:

$$Accuracy = \frac{TP + TN}{TP + TN + FP + FN} \quad (1)$$

Precision

Determines relevant instances from the obtained instances.

$$Precision = \frac{TP}{TP + FP} \quad (2)$$

Recall (sensitivity)

Determines how many true positives there are, divided by the total number of true positives.

$$Recall = \frac{TP}{TP + FN} \quad (3)$$

F1 Score

This result strikes a balance between recall and precision, which means that this is a more accurate way to assess test accuracy.

$$F1Score = \frac{2 * (Precision * Recall)}{Precision + Recall} \quad (4)$$

The below table explains the rest of the other metrics with their formula.

Table 1. Metrics to Evaluate the Model Performance

Measure	Derivations
False Discovery Rate	$FDR = \frac{FP}{FP + TP}$
False Positive Rate	$FPR = \frac{FP}{FP + TN}$
False Negative Rate	$FNR = \frac{FN}{FN + TP}$
Negative Predictive Value	$NPV = \frac{TN}{TN + FN}$
Matthews Correlation Coefficient	$\frac{TP * TN - FP * FN}{\sqrt{(TP + FP) * (TP + FN) * (TN + FP) * (TN + FN)}}$

MobileNetV2

The MobileNetV2 model's classification performance is shown in this section. Since the input for this model must be in the 224 by 224 format, the input photos were downsized to that size. Figure 7 displays the loss and accuracy for the test and validation phases of the MobileNetV2 model before and after Applying the image augmentation techniques. The model's confusion matrix is displayed in Table 2.

Via using 64 picture test data, the MobileNetV2 architecture was assessed. In the testing phase, the model correctly identified 23 out of the 24 images in the class with no brain tumors, and out of the total 40 images for brain tumors, the model correctly identified 39. Sixty-two of these data were effectively classified. The final two test data sets were misclassified.

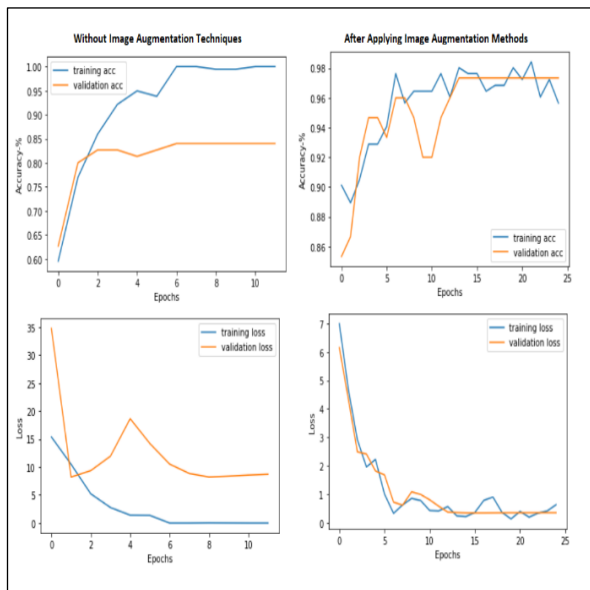


Figure 7. Results of MobileNetV2 before and after Implementing Image Augmentation Approaches

Table 2. Confusion Matrix Produced by MobileNetV2 after Using image Augmentation Techniques

		No Brain Tumor	Brain Tumor
True Classes	No Brain Tumor	23	1
	Brain Tumor	1	39
	Predicted Classes		

VGG19

The VGG19 model's classification performance is shown in this section. Since the input for this model must be in the 224 by 224 format, the input photos were downsized to that size. **Error! Reference source not found.** 8 displays the loss and accuracy for the test and validation phases of the VGG19 model before and after Applying the image augmentation techniques. The model's confusion matrix is displayed in Table 3.

The VGG19 architecture was evaluated using 64-picture test data. Sixty-one of these data were effectively categorized; of the 24 images in the class, no brain tumors were included in the testing phase, the model correctly identified 21 of them, and the model correctly identified all 40 images for brain tumors. The final three test data sets were misclassified.

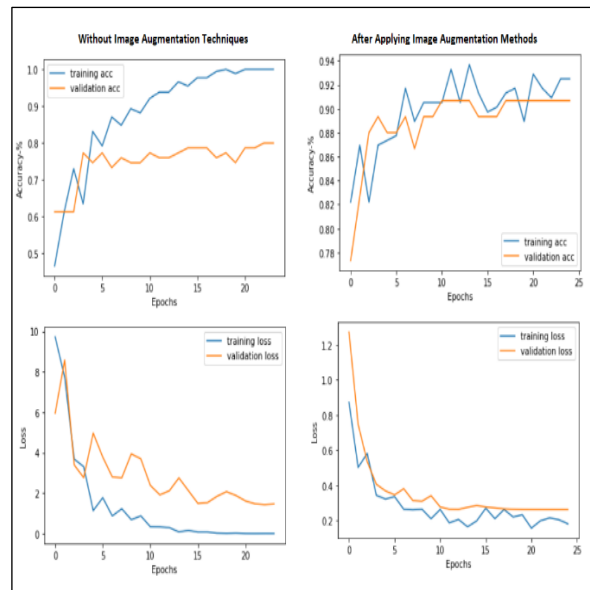


Figure 8. Results of VGG19 before and after Utilizing Image-Enhancing Techniques

DenseNet201

The DenseNet201 model's classification performance is shown in this section. Since the input for this model must be in the 224 by 224 format, the input photos were downsized to that size. Figure 9 displays the loss and accuracy for the test and validation phases of the DenseNet201 model before and after Applying the image augmentation techniques. The model's confusion matrix is displayed in Table 4.

Table 3. VGG19 Confusion Matrix

		No Brain Tumor	Brain Tumor
True Classes	No Brain Tumor	21	3
	Brain Tumor	0	40
	Predicted Classes		

The DenseNet201 architecture was evaluated using 64-picture test data. Sixty of these data were effectively categorized; of the 24 images in the class, no brain tumors were included in the testing phase, the model correctly identified 20 of them, and the model correctly identified all 40 mages for brain tumors. The classification of the final four test data was incorrect.

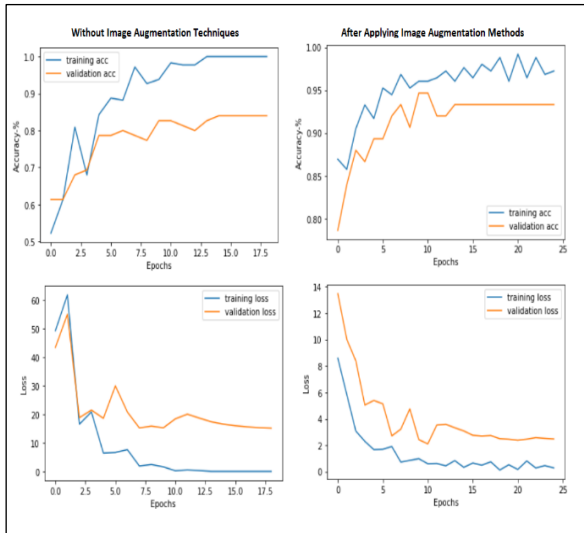


Figure 9. The outcomes of DenseNet201 before and after applying the image augmentation techniques

Table 4. DenseNet201 Confusion Matrix

		No Brain Tumor	Brain Tumor
True Classes	No Brain Tumor	20	4
	Brain Tumor	0	40
Predicted Classes			

Figure 10 explains how image augmentations can aid in detecting and diagnosing brain cancers. Figure 11 explains the false positive and discovery rates for the models. Figure 12 uses several measures to compare the models.

(MobileNetV2, VGG19, and DenseNet201) Overall after using the methods on MRI patients. Table 5 compares the outcomes for the models in terms of accuracy, precision, and f1-score.

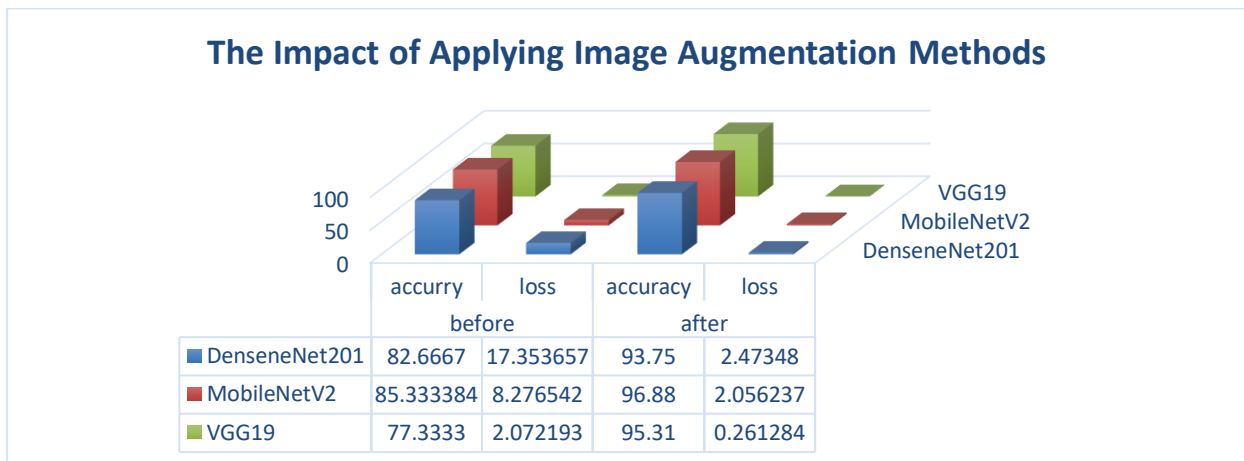


Figure 10. The Impact of Image Enhancement Methods

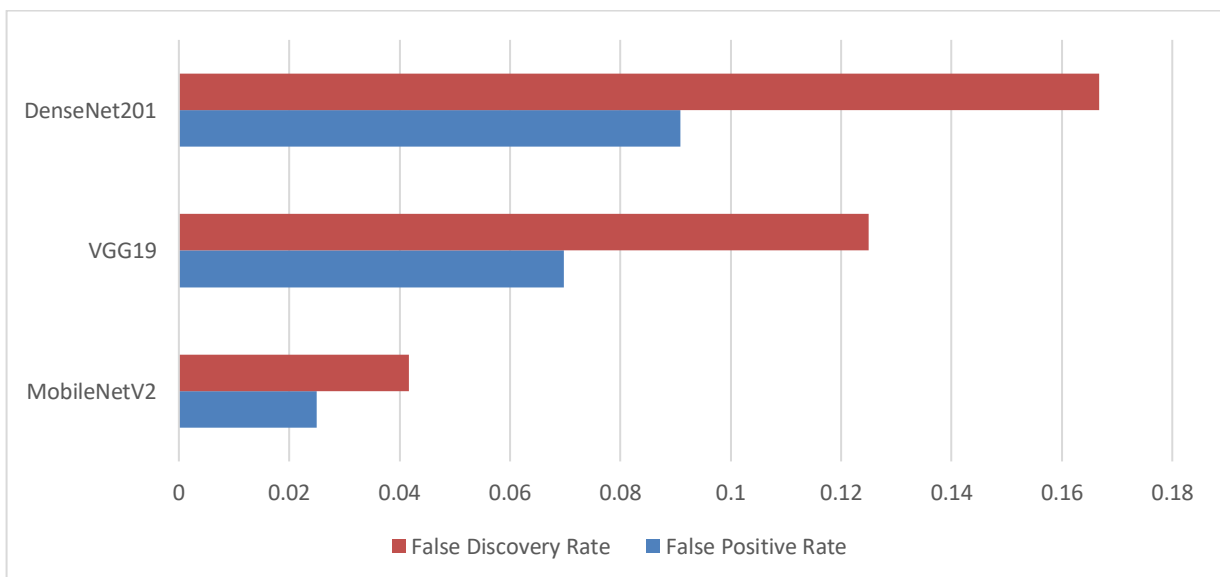


Figure 11. False Positive Rate and False Discovery Rate for the Models

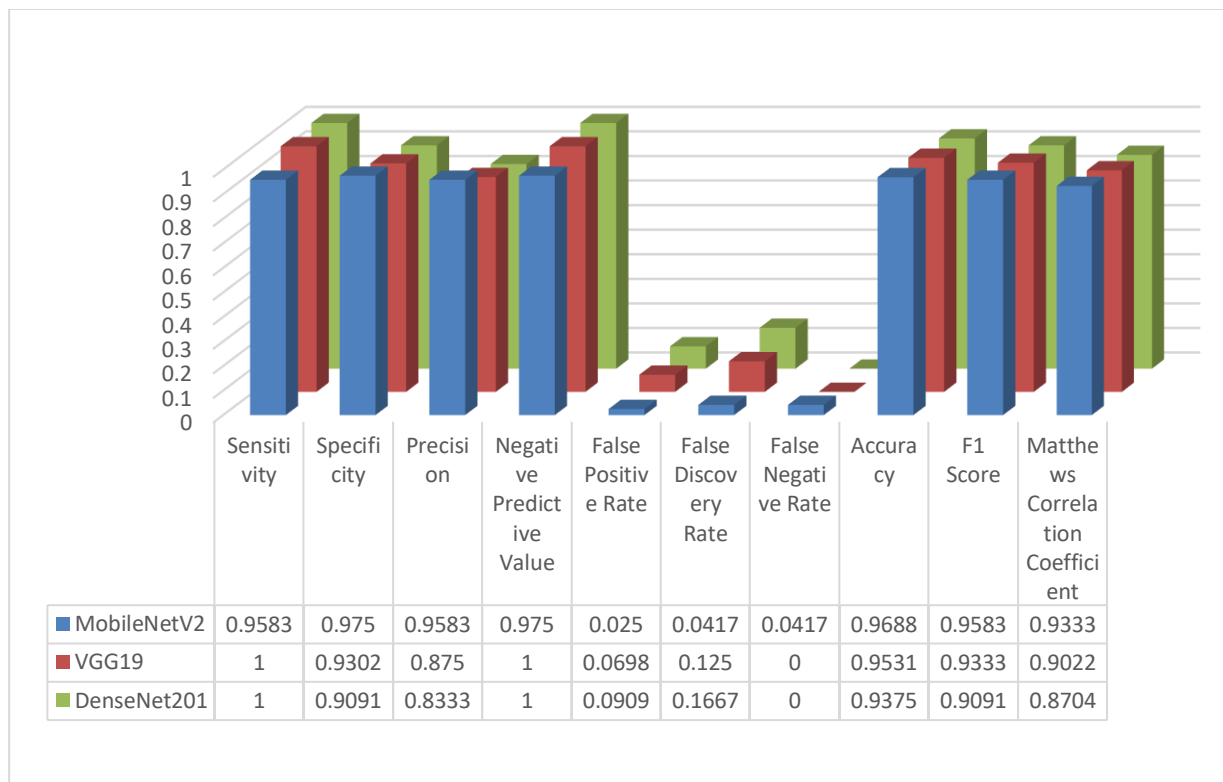


Figure 12. The MobileNetV2, VGG19, and DenseneNet201 Models' Classification Reports

Table 5. Outcomes for the Models in Terms of Accuracy, Precision, and f1-Score.

Models	Accuracy	Precision	F1 score
MobileNetV2	96.88	95.83	95.83
VGG19	95.31	87.5	93.33
DenseNet201	93.75	83.33	90.91

CONCLUSIONS

After using image augmentation techniques, the MobileNetV2 architecture demonstrated the highest accuracy rate during the experiments by 96.88 percent. VGG19 and DenseNet201 architectures achieved an accuracy rate of 95.31% and 93.75%, respectively. To recognize and cure brain cancers, science is still making progress. Finally, the results showed that applying data augmentation approaches improves performance, producing models far better than those trained from scratch.

REFERENCES

[1] S. Chatterjee, F. A. Nizamani, A. Nürnberger, and O. J. S. R. Speck, "Classification of Brain Tumours in MR

Images Using Deep Spatiotemporal Models," *Sci. Rep.*, vol. 12, no. 1, pp. 1–11, 2022.

[2] Y. S. Ismael, M. Y. Shakor, and P. A. Abdalla, "Deep Learning Based Real-Time Face Recognition System," *NeuroQuantology*, vol. 20, no. 6, pp. 7355–7366, 2022.

[3] K. J. Ghafoor, K. M. H. Rawf, A. O. Abdulrahman, and S. H. Taher, "Kurdish Dialect Recognition using 1D CNN", *ARO-The Scientific Journal Of Koya University*, 9(2), pp. 10-14., 2021, doi: 10.14500/aro.10837.

[4] K. H. Rawf, A. Abdulrahman, and A. Mohammed, "Effective Kurdish Sign Language Detection and Classification Using Convolutional Neural Networks," *Res. Sq.*, 2022.

[5] Z. K. Abdul, A. Al-Talabani, and A. O. Abdulrahman, "A New Feature Extraction Technique Based on 1D Local Binary Pattern for Gear Fault Detection," *Shock Vib.*, vol. 2016, pp. 1–6, 2016.

[6] A. A. Mohammed, D. A. Salih, A. M. Saeed, M. Q. Kheder, "An Imperceptible Semi-Blind Image Watermarking Scheme in DWT-SVD Domain Using A Zigzag

- Embedding Technique," *Multimed. Tools Appl.*, vol. 79, pp. 32095–32118, 2020.
- [7] P. A. Abdalla and A. Varol, "Advantages to Disadvantages of Cloud Computing for Small-Sized Business," in *2019 7th International Symposium on Digital Forensics and Security (ISDFS)*, Jun. 2019, vol. 6, no. 6, pp. 1–6.
- [8] P. A. Abdalla and C. Varol, "Testing IoT security: The case study of an ip camera," in *2020 8th International Symposium on Digital Forensics and Security (ISDFS)*, 2020, pp. 1–5.
- [9] K. M. H. Rawf, & A. O. Abdulrahman, "Microcontroller-Based Kurdish Understandable and Readable Digital Smart Clock", *Sci. J. of University of Zakho*, 10(1), 1–4, 2022, <https://doi.org/10.25271/sjuoz.2022.10.1.870>
- [10] A. Raza, H. Ayub, J. A. Khan, I. Ahmad, A. S. Salama, Y. I. Daradkeh, D. Javeed, A. U. Rehman and H. Hamam, "A Hybrid Deep Learning-Based Approach for Brain Tumor Classification," *Electronics*, vol. 11, no. 7, p. 1146, 2022.
- [11] S. Maqsood, R. Damaševičius, and R. Maskeliūnas, "Multi-Modal Brain Tumor Detection Using Deep Neural Network and Multiclass SVM," *Medicina*, vol. 58, no. 8, p. 1090, 2022.
- [12] (2022, 10/10). Brain MRI Images for Brain Tumor Detection. Available: <https://www.kaggle.com/datasets/navoneel/brain-mri-images-for-brain-tumor-detection>
- [13] K. M. H. Rawf, A. A. Mohammed, A. O. Abdulrahman, P. A. Abdalla, K. J. Ghafor, A Comparative Study Using 2D CNN and Transfer Learning to Detect and Classify Arabic-Script-Based Sign Language. *Acta Informatica Malaysia*, vol. 7, no. 1, p. 08-14, 2023
- [14] H. Dong, G. Yang, F. Liu, Y. Mo, and Y. Guo, "Automatic Brain Tumor Detection and Segmentation Using U-Net Based Fully Convolutional Networks," in *annual conference on medical image understanding and analysis*, 2017, pp. 506–517.
- [15] J. Amin, M. Sharif, M. Yasmin, and S. Fernandes, "A Distinctive Approach in Brain Tumor Detection and Classification Using MRI," *Pattern Recognit. Lett.*, vol. 139, pp. 118–127, 2020.
- [16] M.-N. Wu, C.-C. Lin, and C.-C. Chang, "Brain Tumor Detection Using Color-Based K-Means Clustering Segmentation," in *Third international conference on intelligent information hiding and multimedia signal processing (IIH-MSP 2007)*, 2007, vol. 2, pp. 245–250.
- [17] G. R. Chandra and K. R. H. Rao, "Tumor Detection in Brain Using Genetic Algorithm," *Procedia Comput. Sci.*, vol. 79, pp. 449–457, 2016.
- [18] A. B. Olin et al., "Robustness and Generalizability of Deep Learning Synthetic Computed Tomography for Positron Emission Tomography/Magnetic Resonance Imaging-Based Radiation Therapy Planning of Patients with Head and Neck Cancer," *Adv. Radiat. Oncol.*, vol. 6, no. 6, p. 100762, 2021.
- [19] C. Jayachandran Preetha et al., "Deep-Learning-Based Synthesis of Post-Contrast T1-Weighted MRI for Tumour Response Assessment in Neuro-Oncology: A Multicentre, Retrospective Cohort Study," *Lancet Digit. Heal.*, vol. 3, no. 12, pp. e784–e794, 2021.
- [20] S. Amemiya, H. Takao, S. Kato, H. Yamashita, N. Sakamoto, and O. Abe, "Automatic Detection of Brain Metastases on Contrast-Enhanced CT with Deep-Learning Feature-Fused Single-Shot Detectors," *Eur. J. Radiol.*, vol. 136, p. 109577, 2021.
- [21] G. S. Tandel, A. Tiwari and O. G. Kakde, "Performance Optimisation of Deep Learning Models Using Majority Voting Algorithm for Brain Tumour Classification," *Comput. Biol. Med.*, vol. 135, p. 104564, 2021.
- [22] M. Jiang, F. Zhai and J. Kong, "A Novel Deep Learning Model DDU-Net Using Edge Features to Enhance Brain Tumor Segmentation on MR Images," *Artif. Intell. Med.*, vol. 121, p. 102180, 2021.
- [23] S. Namboodiri and P. Arun, "Fingerprint Based Security System for Vehicles," *Int. J. Adv. Res. Ideas Innov. Technol.*, vol. 4, no. 4, pp. 370-372, 2018.
- [24] M. Khairandish, M. Sharma, V. Jain, J. Chatterjee, and N. Z. Jhanjhi, "A Hybrid

- CNN-SVM Threshold Segmentation Approach for Tumor Detection and Classification of MRI Brain Images," *IRBM*, vol. 43, no. 4, pp. 290–299, 2021.
- [25] Z. A. Al-Saffar and T. Yildirim, "A Hybrid Approach Based on Multiple Eigenvalues Selection (MES) for the Automated Grading of A Brain Tumor Using MRI," *Comput. Methods Programs Biomed.*, vol. 201, p. 105945, 2021.
- [26] F. Alonso-Fernandez, J. Fierrez-Aguilar, and J. Ortega-Garcia, "A Review of Schemes for Fingerprint Image Quality Computation," *ArXiv*, vol. 2207.05449, 2022.
- [27] A. Anaya-Isaza and L. Mera-Jiménez, "Data Augmentation and Transfer Learning for Brain Tumor Detection in Magnetic Resonance Imaging," *IEEE Access*, vol. 10, pp. 23217–23233, 2022.
- [28] S. Sharma, R. K. Dudeja, G. S. Auja, R. S. Bali and N. Kumar, "DeTrAs: deep learning-based healthcare framework for IoT-based assistance of Alzheimer patients," *Neural Comput. Appl.*, pp. 1–13, 2020.
- [29] P. Abdalla, A. Mohammed, O. J. Rasheed, S. H. T. Karim, B. A. Mohammed, and K. J. Ghafoor, "Transfer Learning Models Comparison for Detecting and Diagnosing Skin Cancer," *Acta Inform. Malaysia*, vol. 7, no. 1, pp. 1–7, 2022.
- [30] S. A. Althubiti, F. Alenezi, S. Shitharth, S. K., and C. V. S. Reddy, "Circuit Manufacturing Defect Detection Using VGG16 Convolutional Neural Networks," *Wirel. Commun. Mob. Comput.*, vol. 2022, pp. 1–10, 2022.
- [31] S.-H. Wang and Y.-D. Zhang, "DenseNet-201-Based Deep Neural Network with Composite Learning Factor and Precomputation for Multiple Sclerosis Classification," *ACM Trans. Multimed. Comput. Commun. Appl.*, vol. 16, no. 2s, pp. 1–19, 2020.
- [32] A. Luque, A. Carrasco, A. Martín, and A. de las Heras, "The Impact of Class Imbalance in Classification Performance Metrics Based on the Binary Confusion Matrix," *Pattern Recognit.*, vol. 91, no. 2s, pp. 216–231, 2019.
- [33] M. S. Junayed et al., "AcneNet - A Deep CNN Based Classification Approach for Acne Classes," in *2019 12th International Conference on Information & Communication Technology and System (ICTS)*, Jul. 2019, vol. 91, no. 2s, pp. 203–208.